The Quest for an Accurate Functional Tumor Volume with ^{68}Ga-DOTATATE PET/CT

Ryan P. Reddy[1], C. Ross Schmidtlein[1], Romina G. Giancipoli[2], Audrey Mauguen[3], Daniel LaFontaine[1], Heiko Schoder[1], and Lisa Bodei[1]

[1]*Molecular Imaging and Therapy Service, Department of Radiology, Memorial Sloan Kettering Cancer Center, New, York, New York;* [2]*Department of Nuclear Medicine, La Sapienza University of Rome, Rome, Italy; and* [3]*Department of Epidemiology and Biostatistics, Memorial Sloan Kettering Cancer Center, New York, New York*

^{68}Ga-labeled somatostatin analog (SSA) PET/CT is now a standard-of-care component in the management of neuroendocrine tumors (NETs). However, treatment response for NETs is still assessed with morphologic size measurements from other modalities, which can result in inaccuracy about the disease burden. Functional tumor volume (FTV) acquired from SSA PET/CT has been suggested as a possible metric, but no validated measurement tool to measure FTV exists. We tested the precision of multiple FTV computational approaches compared with morphologic volume measurements to identify a candidate for incorporation into future FTV studies to assess tumor burden more completely and accurately. **Methods:** The clinical and imaging data of 327 NET patients were collected at Memorial Sloan Kettering Cancer Center between December 2016 and April 2018. Patients were required to have SSA PET/CT and dedicated CT scans within 6 wk and were excluded if they had any intervention between scans. When paired studies were evaluated, 150 correlating lesions demonstrated SSA. Lesions were excluded if they contained necrotic components or were lobulated. This exclusion resulted in 94 lesions in 20 patients. The FTV for each lesion was evaluated with a hand-drawn assessment and 3 automated techniques: 50% threshold from SUV_{max}, 42% threshold from SUV_{max}, and background-subtracted lesion activity. These measurements were compared with volume calculated from morphologic volume measurements. **Results:** The FTV calculation methods showed varying correlations with morphologic volume measurements. FTV using a 42% threshold had a 0.706 correlation, hand-drawn volume from PET imaging had a 0.657 correlation, FTV using a 50% threshold had a 0.645 correlation, and background-subtracted lesion activity had a 0.596 correlation. The Bland–Altman plots indicated that all FTV methods had a positive mean difference from morphologic volume, with a 50% threshold showing the smallest mean difference. **Conclusion:** FTV determined with thresholding of SUV_{max} demonstrated the strongest correlation with traditional morphologic lesion volume assessment and the least bias. This method was more accurate than FTV calculated from hand-drawn volume assessments. Threshold-based automated FTV assessment promises to better determine disease extent and prognosis in patients with NETs.

Key Words: functional tumor volume; neuroendocrine tumors; somatostatin analogs; PET/CT

J Nucl Med 2022; 63:1027–1032
DOI: 10.2967/jnumed.121.262782

Neuroendocrine tumors (NETs) encompass a group of diverse neoplasms that typically originate from the gastrointestinal tract, the pancreas, and the bronchopulmonary tract. Although they can have varying presentations, they have similar histopathologic features and may secrete biologically active compounds (*1*). Given a general lack of awareness of NETs and their slow-growing nature, diagnosis is missed 20%–40% of the time or is made only at a later stage because of detectable findings such as tumor mass effects or biomarker secretions. At this stage, metastatic disease is typically present, and curative options are no longer feasible (*2*). Common treatments include locoregional treatments and conventional chemotherapy. Recently, peptide receptor radionuclide therapy with radiolabeled somatostatin analogs (SSAs) has been approved as an additional treatment option for inoperable or metastatic gastroenteropancreatic NETs (*2,3*).

Imaging plays a pivotal role in diagnosis, staging, treatment selection, and follow-up of NETs (*4*). A combination of somatostatin receptor imaging and morphologic cross-sectional CT or MRI is now performed to acquire all clinically relevant information. Somatostatin receptor imaging targets the high density of somatostatin receptors that predominate on the cell membranes of low-grade NETs. In recent years, the use of PET/CT with ^{68}Ga-labeled SSAs, such as ^{68}Ga-DOTATATE PET/CT, has demonstrated sensitivity and resolution superior to that of conventional ^{111}In-octreotide scanning. This modality is now Food and Drug Administration–approved, has become an accepted standard-of-care imaging modality (*5–7*), and has substantially improved the identification and management of NETs.

Despite the introduction of SSA PET/CT, the clinical and research response of NETs to treatment is still assessed with morphologic size measurements, such as RECIST 1.1, that are obtained solely with CT and MRI. Morphologic assessment can exclude many sites of disease identifiable only on SSA PET/CT. Additionally, morphologic size measurements have limited applicability for slow-growing lesions such as NETs. This can result in underestimation of therapeutic effects and can inaccurately bias management decisions (*8–10*). Some lesion assessments, such as the Choi criteria, attempt to correct for these variables, but the dependance on CT or MRI still limits disease assessment for many patients with low-grade NETs (*11–13*).

Because the inclusion of SSA PET/CT better evaluates the full extent of NET disease, a measurement technique using these PET imaging data can provide a more complete and accurate disease assessment for NETs. Prior literature has suggested that functional

Received Jul. 1, 2021; revision accepted Oct. 25, 2021.
For correspondence or reprints, contact Ryan P. Reddy (reddyr@mskcc.org).
Published online Nov. 12, 2021.

tumor volume (FTV) is a possible suitable metric (*14,15*) and has shown promise of prognostic utility for FTV in NETs (*15–19*). However, no validated approach has yet been developed to calculate FTV in SSA PET/CT imaging. In prior investigations, the method to calculate FTV has varied and was often chosen arbitrarily on the basis of prior approaches and techniques with ^{18}F-FDG PET/CT. For example, Abdulrezzak et al. (*16*) and Toriihara et al. (*17*) used a 50% threshold of SUV_{max}, Ohnana et al. (*18*) used a 41% threshold of SUV_{max}, and Tirosh et al. (*15*) used a patient-customized method to subtract background uptake.

The development and validation of an algorithm or analytic process that most accurately measures FTV using SSA PET/CT imaging data would help standardize these prognostic assessments and more accurately identify the full extent of low-grade NET disease, which can be indolent on CT or MRI. This standardization could help create a more reproducible and accurate biomarker to identify patients most at risk for disease progression and to help manage treatment decisions.

We have selected some of the techniques previously used to compute tumor volume from SSA PET/CT to assess which method best approximates and correlates with morphologic size measurements, which are the current standard of practice. One of these measurement techniques is computing tumor volume using a threshold (ranging from 40% to 50%) related to the respective lesion's SUV_{max} to remove background uptake (*20*). We chose to test thresholds of 42% and 50%, as these have been used in prior studies evaluating tumor volume for both ^{18}F-FDG PET/CT and SSA PET/CT. Another method uses customized background-based estimation—including background-subtracted lesion activity (BSL)—that surrounds each lesion with a single volume of interest (VOI) and then analyzes the resultant histogram of that VOI to remove any background uptake for each lesion (*21,22*). In this study, our aim was to evaluate these different FTV measurement methods with SSA PET/CT and compare these results with lesion volumes calculated from morphologic size measurements.

MATERIALS AND METHODS

Patient and Lesion Selection

The institutional review board approved this retrospective single-center study and waived the informed consent requirement.

The Memorial Sloan Kettering Cancer Center (MSKCC) GE Healthcare PACS was retrospectively searched for patients who had undergone ^{68}Ga-DOTATATE PET/CT between December 2016 and May 2018. This search identified 327 patients with NETs cared for by our service. The clinical, histopathologic, and imaging data of these patients were obtained and organized. We then restricted our population to the 211 patients who had undergone both ^{68}Ga-DOTATATE PET/CT and contrast-enhanced CT.

Additional clinical data were used to include only patients with both a ^{68}Ga-DOTATATE PET/CT and a triphasic contrast-enhanced CT examination within 6 wk of each other. Also, to ensure that all lesions demonstrated somatostatin avidity, the study included only patients whose dictated nuclear medicine and radiology reports shows concordant findings of neoplastic disease on SSA PET/CT and CT. In addition, patients were excluded if they had any therapeutic intervention between their SSA PET/CT and CT examinations. These criteria resulted in 25 patients with paired SSA PET/CT and CT examinations and concurrent findings.

The paired ^{68}Ga-DOTATATE PET/CT and contrast-enhanced CT examinations were evaluated; 150 lesions showed SSA uptake and were clearly identifiable in all planes on CT imaging. Lesions were then excluded if they either contained necrotic components or were lobulated, as an accurate morphologic volume would be difficult to calculate for these types of lesions from traditional morphologic size assessments. Additionally, 1 lesion was excluded because no biopsy results were obtained during that patient's care at MSKCC. This exclusion resulted in 94 clearly identifiable lesions from 20 patients. Each of these ellipsoid lesions demonstrated a precise correlation between the PET imaging and the contrast-enhanced CT imaging in all dimensions.

Diagnostic Imaging Acquisition Protocols

All patients were examined with the routine ^{68}Ga-DOTATATE PET/CT clinical protocol on a GE Healthcare Discovery 690 or 710 PET/CT scanner. Both scanners use the same PET acquisition hardware and software. Each patient received an intravenous injection of ^{68}Ga-DOTATATE with a mean injected activity of 193.51 MBq (range, 166.5–203.5 MBq) and were scanned after an average 64-min delay (range, 60–75 min). The low-dose, unenhanced CT sequence and PET sequence were obtained from the mid skull to the upper thighs. The SUVs were normalized to the patient's body weight. All PET/CT scanners used at MSKCC are cross-calibrated for the SUV measurement, allowing a valid comparison between SUV_{max} measurements made on different scanners.

All patients were also examined with separate triple-phase contrast-enhanced CT examinations performed with the routine MSKCC clinical protocol. After oral and intravenous iodinated contrast administration, multislice helical sections were obtained from the thoracic inlet to the pubic symphysis. Imaging of the abdomen included a precontrast phase, a timed arterial phase imaged 35 s after contrast injection, and a timed portal phase imaged 80 s after contrast injection.

FTV Quantification Analysis

The FTV was determined as the sum of all voxels, within the identified VOI, whose uptake matched a predetermined guideline. All FTV measurements and analyses were performed using VolumeShare software, version 7, for the Advantage Workstation (GE Healthcare). Initially, a VOI was created to encircle each identifiable lesion on the ^{68}Ga-DOTATATE PET/CT scan. Each VOI was created to select only a single lesion and to minimize the amount of physiologically elevated background uptake surrounding each lesion within the VOI.

Then, a hand-drawn volume was created to circumscribe each lesion, using each lesion's visible tumor activity as seen on the diagnostic PET images and excluding any surrounding regions of physiologically increased background activity.

The initial VOI of each lesion was then used to calculate the FTV using thresholds. The first method summed the voxels that demonstrated uptake matching or exceeding a threshold percentage of the lesion's SUV_{max}. For this method, 2 different thresholds were evaluated, 42% and 50%.

Lastly, the BSL method was performed (*21,22*). For each lesion, the imaging data from the initial VOI were transposed into a histogram to calculate the BSL activity. The histograms represent the voxels of the VOI as a function of SUVs. Then, the background activity surrounding the lesion was removed by subtracting a gaussian fit over the peak of the VOI's histogram. Any negative values were reset to zero. The remaining positive values in the histogram could be summed to calculate the FTV based on BSL.

To establish a reference standard for lesion volume, the contrast-enhanced CT examinations were used to measure the morphologic volume of each lesion using the GE Healthcare PACS. Each lesion was measured manually in 3 dimensions using the arterial and venous phase sequences. For each lesion, the longest diameter on segmented axial images was measured, followed by the longest perpendicular diameter. A third, craniocaudal, diameter was then measured using

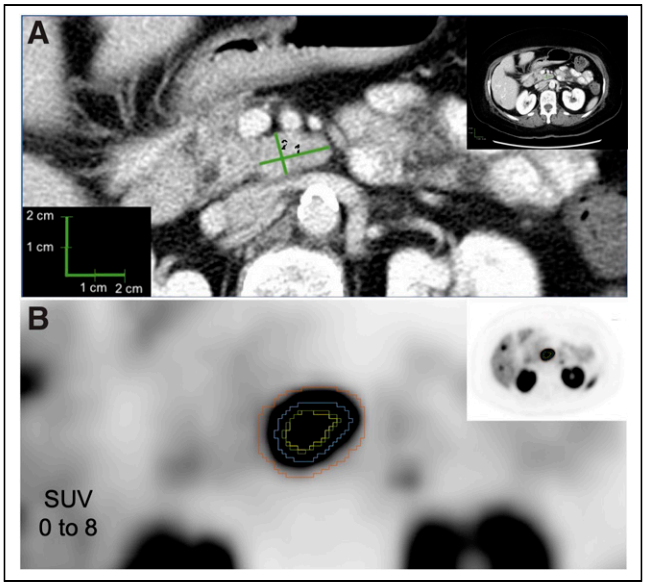

FIGURE 1. Example lesion 1. (A) CT evaluation of lymph node, with longest diameter of 2.2 cm (1) and longest perpendicular diameter of 1.3 cm (2). (B) PET evaluation of lymph node, with yellow representing 50% threshold segmentation; green, 42% threshold segmentation; blue, manual segmentation; and red, BSL segmentation.

segmented sagittal or coronal imaging sequences. Since only ellipsoidal lesions were included, the morphologic volume could be calculated as $\frac{4}{3}\ \pi abc$. Figures 1 and 2 demonstrate example lesions with their calculated FTVs and morphologic volumes.

Statistical Analysis

The Pearson correlation coefficient was used to evaluate the correlation of morphologic lesion volume with the 4 approaches to FTV assessment. Linear models with a random intercept were used to account for

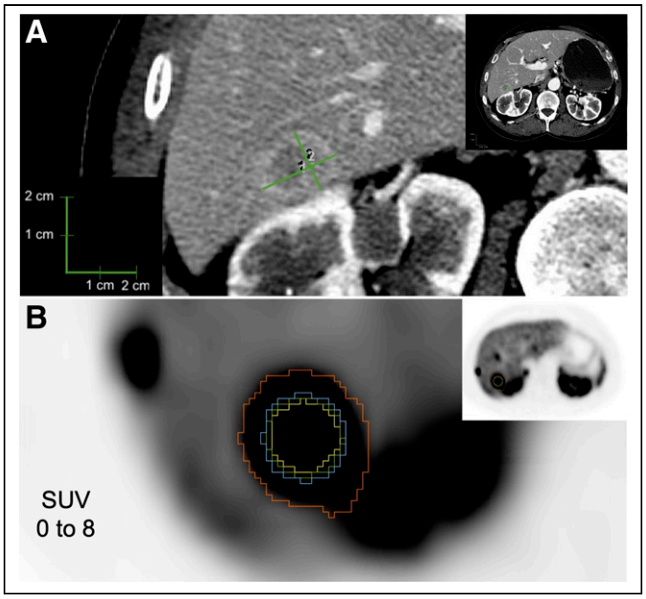

FIGURE 2. Example lesion 2. (A) CT evaluation of hepatic metastasis, with longest diameter of 2.3 cm (1) and longest perpendicular diameter of 1.8 cm (2). (B) PET evaluation of hepatic metastasis, with yellow representing 50% threshold segmentation; green, 42% threshold segmentation; blue, manual segmentation; and red, BSL segmentation.

TABLE 1
Demographic and Histopathologic Data

Characteristic	Data
Patients	20 (100%)
Sex	
Female	13 (65%)
Male	7 (35%)
Age at ^{68}Ga-DOTATATE PET (y)	
Mean ± SD	56 ± 12
Range	28–78
NET primary tumor subtype (%)	
Pancreatic	11 (55%)
Small intestine	5 (25%)
Other	3 (15%)
Unknown	1 (5%)
Gastroenteropancreatic NET grade	
G1 (Ki-67 < 3%)	5 (29%)
G2 (Ki-67 = 3%–20%)	9 (53%)
G3 (Ki-67 > 20%)	3 (18%)
Local recurrence	1 (5%)
Metastases	
No	2 (10%)
Yes	18 (90%)
Metastatic sites	
Liver	18
Nodes	8
Bone	3
Adrenal	2
Mesenteric	2
Cardiac	1
Splenic	1
Clinical syndrome	
Nonfunctioning tumor	12 (60%)
Functioning tumor	8 (40%)

Data are number, except for age.

TABLE 2
Medical and Surgical Treatments Before Imaging

Treatment	*n*
Resection of primary tumor	9 (45%)
Additional treatments	
Liver-directed therapy	7 (35%)
Chemotherapy	4 (20%)
Radiotherapy	1 (5%)
Peptide radionuclide receptor therapy	0
Treatment with cold SSA at time of ^{68}Ga-DOTATATE PET/CT	8 (40%)

TABLE 3
^{68}Ga-DOTATATE–Avid Lesion Locations and Measurements

Parameter	Data
SUV_{max}	
Mean ± SD	36.9 ± 27.0
Range	1.3–188.3
Lesions analyzed	94
Site of lesions	
Liver	69 (73.4%)
Node	10 (10.6%)
Pancreas	5 (5.3%)
Bone	5 (5.3%)
Bowel	2 (2.1%)
Perihepatic implant	2 (2.1%)
Mesenteric node	1 (1.1%)

Data are number, except for SUV_{max}.

any intrapatient correlation between lesions from the same patient. Additionally, the FTVs measured by the 4 approaches were statistically compared with morphologic volume by the included Bland–Altman plots. A log transformation for the Bland–Altman plots was used to correct the skewness in the distribution of the volumes.

RESULTS

Of the 20 patients, 65% were women and 35% were men. The mean age (±SD) at the time of PET scanning was 56 ± 12 y. The primary tumor sites included pancreas for 11 patients (55%) and small intestine for 5 patients (25%). There was 1 patient with an unknown primary (5%). Additionally, there were 2 patients with a gastric primary and 1 patient with a renal primary (Table 1).

Metastases were detected in 18 patients (90%). The most common metastatic site was the liver, with 18 patients (90%). Other common sites of metastasis were nodal for 8 patients (40%) and bone for 3 patients (15%). A single patient had a local recurrence. Additionally, 2 patients had adrenal metastasis, 2 had mesenteric metastasis, 1 had cardiac metastasis, and 1 had splenic metastasis (Table 1).

According to the 2019 World Health Organization classification grading system, 5 patients (29%) with gastroenteropancreatic NETs had G1 tumors (Ki-67 < 3%), 9 (53%) had G2 tumors (Ki-67 = 3%–20%), and 3 (18%) had G3 tumors (Ki-67 > 20%). Three patients had NET carcinoid tumors without Ki-67 information (Table 1).

Only 8 patients had a clinical syndrome (diarrhea or flushing) at the time of the diagnosis, and only 8 patients were under treatment with cold SSAs at the time of SSA PET/CT imaging. The patients had undergone a variety of prior treatments, including primary resection in 9 patients, liver-directed therapies in 7, chemotherapy in 4, and radiotherapy in 1 (Table 2).

In total, 94 lesions were analyzed for FTV. The mean SUV_{max} of the lesions was 36.9 ± 27.0. Most lesions were in the liver (69). Additional sites of lesions included the lymph nodes (10), pancreas (5), bones (5), small bowel (2), and mesentery (1), as well as a perihepatic implant (2) (Table 3).

The different FTV calculation methods demonstrated varying correlations to morphologic volume measurements for the full population of 94 lesions. Calculating FTV using the 42% threshold provided a 0.706 correlation. The hand-drawn volume from the PET imaging provided a 0.657 correlation. The method using 50% thresholding had a 0.645 correlation, and the BSL method had a 0.596 correlation (Fig. 3).

The Bland–Altman plots (Fig. 4) were well distributed across 0 for each FTV calculation method, but all 4 FTV methods had positive mean difference when compared with morphologic volume. The FTV calculated using 50% thresholding showed the smallest mean difference. This difference between FTV methods and the morphologic volume is not affected by the size of the lesion.

DISCUSSION

In our study, we evaluated different methods to calculate FTV from SSA PET/CT and compared these with morphologic volumes. An FTV calculated using thresholding methods related to SUV_{max} outperformed other techniques and may more completely

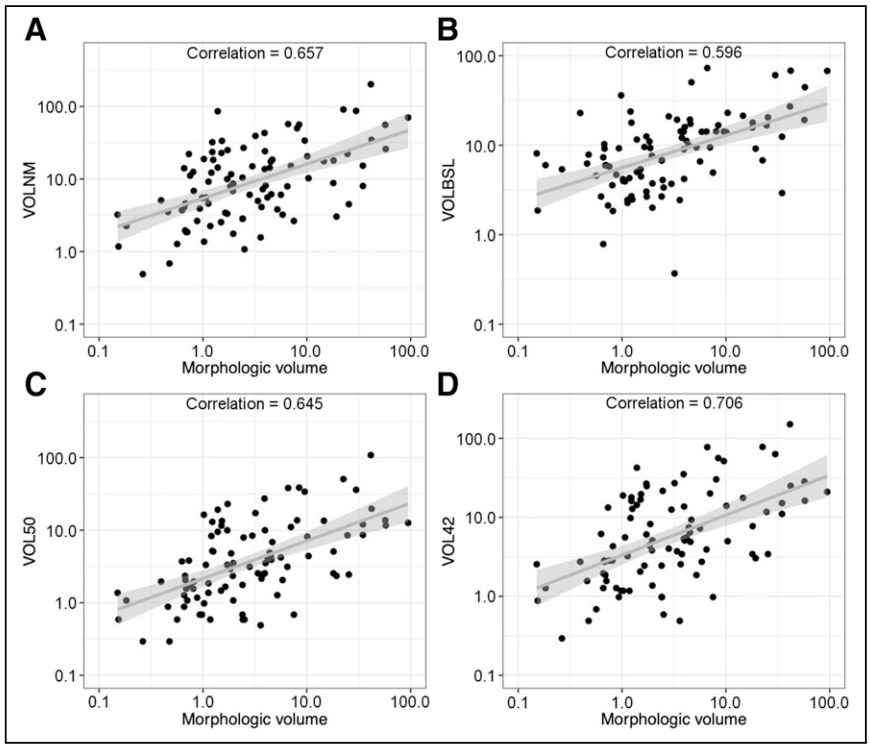

FIGURE 3. Correlation charts of FTV calculations to morphologic measurements. (A) Manual volume from PET imaging (VOLNM). (B) BSL (VOLBSL). (C) Threshold of 50% relative to SUV_{max} (VOL50). (D) Threshold of 42% relative to SUV_{max} (VOL42).

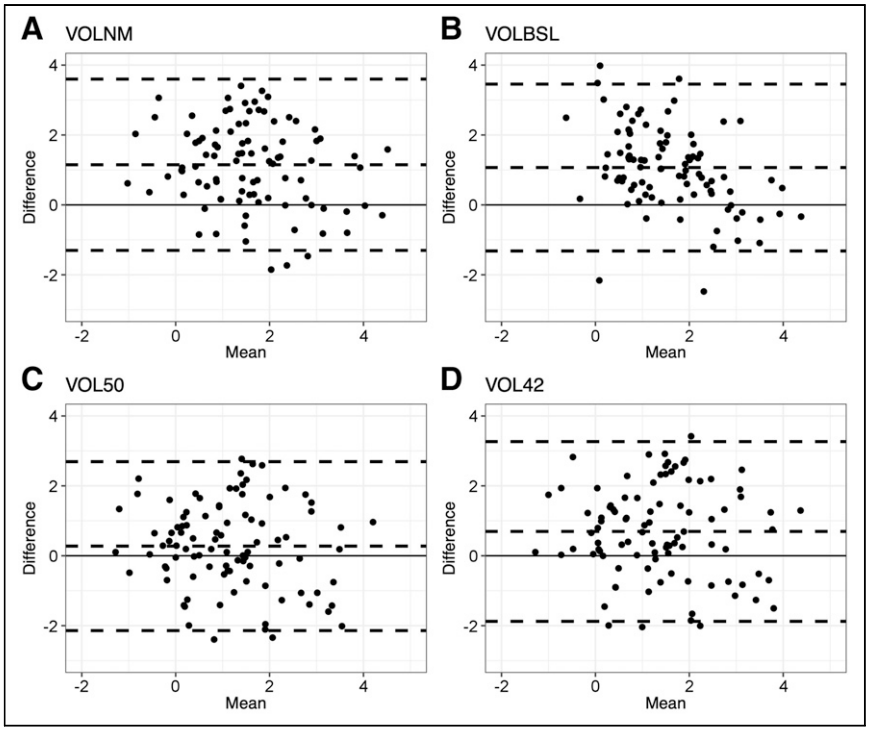

FIGURE 4. Bland–Altman scatterplots showing relative difference between FTV method as labeled and morphologic volume on *y*-axis and mean volume of FTV method as labeled and morphologic volume on *x*-axis. Dashed lines represent upper limits of agreement, lower limits of agreement, and bias (or mean difference). Log transformation was used to correct skewness in distribution of volumes. (A) Manual volume from PET imaging (VOLNM). (B) BSL (VOLBSL). (C) Threshold of 50% relative to SUV_{max} (VOL50). (D) Threshold of 42% relative to SUV_{max} (VOL42).

and accurately assess tumor burden for NETs than traditional morphologic assessments.

Since the arrival of SSA PET/CT into the clinical sphere, there have been attempts to understand how to best use it for patient management. Some have suggested that FTV may represent a better correlation with prognosis than SUV_{max} by better capturing extent of disease and response to therapy (*14–19*). But because there is no consensus or validated FTV method with SSA PET/CT, we appropriated some previously used FTV methods. These include SUV_{max} thresholding methods related to SUV_{max}, hand-drawn volumes, and a BSL method described in prior published studies by MSKCC.

Use of the hand-drawn volumes for calculation of FTV performed favorably, with a strong correlation to the morphologic volume. Unfortunately, this technique also consistently demonstrated the largest overestimation of lesion size compared with morphologic volume. It is unclear whether this bias is due to the companion CT images of the PET examination. An additional major limitation of this method is the time required to manually circumscribe each lesion.

Although the FTV calculation based on the BSL technique showed promise for ^{18}F-FDG PET/CT in prior studies, we demonstrated that this technique performed poorly for SSA PET/CT. This technique had the lowest correlation between calculated FTV and morphologic volume. Additionally, this technique greatly overestimated lesion size compared with morphologic volume, suggesting that the distribution of SSA uptake from the background parenchyma cannot be completely estimated by a classic gaussian distribution.

Both FTVs computed on the basis of SUV_{max} thresholds showed strong correlations with morphologic lesion volume, as well as showing the smallest overall differences from morphologic lesion volume. The 42% threshold had the strongest correlation with morphologic volume, including the hand-drawn volume, and the second smallest mean difference. The 50% threshold demonstrated the smallest mean difference from morphologic volume, or the smallest overestimation, and the third strongest correlation with morphologic volume. This result suggests that an FTV with thresholding values may be the best candidate for an FTV measurement technique to assess tumor burden for low-grade NETs. Because use of the 42% and 50% thresholds was arbitrarily chosen given their prior use for tumor volume assessments in the literature, a threshold set to a different percentage could demonstrate a stronger correlation with morphologic tumor volume, with less bias or overestimation. As the 50% threshold with least bias demonstrated a lower correlation than the 42% threshold, it is possible that a second variable is needed to adjust FTV to best approximate morphologic volume. These results suggest that more inquiry is likely needed to answer these questions.

The main limitation of our study was our exclusion of lesions with necrotic components and with more complex 3-dimensional volumes. These were excluded because of the difficulty of calculating an accurate morphologic volume for these lesions via CT imaging. Future studies are needed to evaluate whether an FTV method based on an SUV_{max} threshold can be used to accurately measure the SSA-positive portions of these types of NET lesions.

CONCLUSION

Because SSA PET/CT can better evaluate the full extent of NET disease than CT or MRI, a measurement technique using these PET imaging data can provide a more complete and accurate assessment of total disease. Our study demonstrated a strong correlation between FTV calculated using SUV_{max} thresholding and traditional morphologic lesion volumes. Measurements were also more accurate using this method than using morphologic lesion volumes. Additionally, this method was more accurate than FTV calculated from hand-drawn volume assessments. This FTV assessment technique is the best candidate for future evaluation and for incorporation of total-body tumor volume algorithms to more completely and accurately assess tumor burden and prognosis for NET patients.

DISCLOSURE

This research was funded in part through NIH/NCI Cancer Center Support Grant P30 CA008748. Ryan Reddy is a nonremunerated consultant for AAA-Novartis and Curium. Lisa Bodei is a nonremunerated consultant/speaker for AAA-Novartis, Ipsen, ITM, Curium, Clovis Oncology, Iba, and MTTI and received a

research grant from AAA-Novartis. No other potential conflict of interest relevant to this article was reported.

KEY POINTS

QUESTION: What is the best FTV measurement method for ^{68}Ga SSA PET/CT imaging of NETs?

PERTINENT FINDINGS: We found a strong correlation and the smallest bias between FTV and traditional morphologic lesion volume when using an SUV_{max} threshold on SSA PET/CT. Additionally, this method of computation outperformed FTV calculated from hand-drawn volume assessments with regard to accuracy.

IMPLICATIONS FOR PATIENT CARE: FTV assessment based on an SUV_{max} threshold is a promising basis for more accurate measurement of tumor volume and should be further studied to create FTV algorithms to better determine the extent of disease and the prognosis.

REFERENCES

1. Wang HY, Li ZW, Sun W, et al. Automated quantification of Ki-67 index associates with pathologic grade of pulmonary neuroendocrine tumors. *Chin Med J.* 2019;132:551–561.
2. Bodei L, Kwekkeboom DJ, Kidd M, Modlin IM, Krenning EP. Radiolabeled somatostatin analogue therapy of gastroenteropancreatic cancer. *Semin Nucl Med.* 2016;46:225–238.
3. Strosberg J, El-Haddad G, Wolin E, et al. Phase 3 trial of ^{177}Lu-Dotatate for midgut neuroendocrine tumors. *N Engl J Med.* 2017;376:125–135.
4. Bodei L, Sundin A, Kidd M, Prasad V, Modlin IM. The status of neuroendocrine tumor imaging: from darkness to light? *Neuroendocrinology.* 2015;101:1–17.
5. Geijer H, Breimer LH. Somatostatin receptor PET/CT in neuroendocrine tumours: update on systematic review and meta-analysis. *Eur J Nucl Med Mol Imaging.* 2013;40:1770–1780.
6. Kazmierczak PM, Rominger A, Wenter V, et al. The added value of ^{68}Ga-DOTATATE-PET to contrast-enhanced CT for primary site detection in CUP of neuroendocrine origin. *Eur Radiol.* 2017;27:1676–1684.
7. Hofman MS, Kong G, Neels OC, Eu P, Hong E, Hicks RJ. High management impact of Ga-68 DOTATATE (GaTate) PET/CT for imaging neuroendocrine and other somatostatin expressing tumours. *J Med Imaging Radiat Oncol.* 2012;56:40–47.
8. Yao JC, Shah MH, Ito T, et al. Everolimus for advanced pancreatic neuroendocrine tumors. *N Engl J Med.* 2011;364:514–523.
9. Pavel ME, Hainsworth JD, Baudin E, et al. Everolimus plus octreotide long-acting repeatable for the treatment of advanced neuroendocrine tumours associated with carcinoid syndrome (RADIANT-2): a randomised, placebo-controlled, phase 3 study. *Lancet.* 2011;378:2005–2012.
10. Raymond E, Dahan L, Raoul JL, et al. Sunitinib malate for the treatment of pancreatic neuroendocrine tumors. *N Engl J Med.* 2011;364:501–513.
11. de Mestier L, Dromain C, d'Assignies G, et al. Evaluating digestive neuroendocrine tumor progression and therapeutic responses in the era of targeted therapies: state of the art. *Endocr Relat Cancer.* 2014;21:R105–R120.
12. Solis-Hernandez MP, Fernandez Del Valle A, Carmona-Bayonas A, et al. Evaluating radiological response in pancreatic neuroendocrine tumours treated with sunitinib: comparison of Choi versus RECIST criteria (CRIPNET_ GETNE1504 study). *Br J Cancer.* 2019;121:537–544.
13. Luo Y, Chen J, Huang K, et al. Early evaluation of sunitinib for the treatment of advanced gastroenteropancreatic neuroendocrine neoplasms via CT imaging: RECIST 1.1 or Choi criteria? *BMC Cancer.* 2017;17:154.
14. Baum RP, Kulkarni HR. THERANOSTICS: from molecular imaging using Ga-68 labeled tracers and PET/CT to personalized radionuclide therapy—the Bad Berka experience. *Theranostics.* 2012;2:437–447.
15. Tirosh A, Papadakis GZ, Millo C, et al. Prognostic utility of total ^{68}Ga-DOTATATE-avid tumor volume in patients with neuroendocrine tumors. *Gastroenterology.* 2018;154:998–1008.e1.
16. Abdulrezzak U, Kurt YK, Kula M, Tutus A. Combined imaging with ^{68}Ga-DOTATATE and ^{18}F-FDG PET/CT on the basis of volumetric parameters in neuroendocrine tumors. *Nucl Med Commun.* 2016;37:874–881.
17. Toriihara A, Baratto L, Nobashi T, et al. Prognostic value of somatostatin receptor expressing tumor volume calculated from ^{68}Ga-DOTATATE PET/CT in patients with well-differentiated neuroendocrine tumors. *Eur J Nucl Med Mol Imaging.* 2019;46:2244–2251.
18. Ohnona J, Nataf V, Gauthe M, et al. Prognostic value of functional tumor burden on ^{68}Ga-DOTATOC PET/CT in patients with pancreatic neuro-endocrine tumors. *Neoplasma.* 2019;66:140–148.
19. Ohlendorf F, Henkenberens C, Brunkhorst T, et al. Volumetric ^{68}Ga-DOTA-TATE PET/CT for assessment of whole-body tumor burden as a quantitative imaging biomarker in patients with metastatic gastroenteropancreatic neuroendocrine tumors. *Q J Nucl Med Mol Imaging.* April 14, 2020 [Epub ahead of print].
20. Foster B, Bagci U, Mansoor A, Xu Z, Mollura DJ. A review on segmentation of positron emission tomography images. *Comput Biol Med.* 2014;50:76–96.
21. Burger IA, Vargas HA, Apte A, et al. PET quantification with a histogram derived total activity metric: superior quantitative consistency compared to total lesion glycolysis with absolute or relative SUV thresholds in phantoms and lung cancer patients. *Nucl Med Biol.* 2014;41:410–418.
22. Burger IA, Casanova R, Steiger S, et al. ^{18}F-FDG PET/CT of non-small cell lung carcinoma under neoadjuvant chemotherapy: background-based adaptive-volume metrics outperform TLG and MTV in predicting histopathologic response. *J Nucl Med.* 2016;57:849–854.